arXiv:cond-mat/0306065v1 [cond-mat.soft] 3 Jun 2003

Dynamics of rigid and flexible extended bodies in viscous films and membranes

Alex J. Levine[1,2], T.B. Liverpool[1,3] and F.C. MacKinstosh[1,4]
[1] *The Kavli Institute for Theoretical Physics, University of California, Santa Barbara CA 93106*
[2] *Department of Physics, University of Massachusetts, Amherst Amherst MA 01060*
[3] *Department of Applied Mathematics, University of Leeds, Leeds, LS2 9JT, United Kingdom and*
[4] *Division of Physics & Astronomy, Vrije Universiteit 1081 HV Amsterdam, The Netherlands*
(Dated: February 2, 2008)

We study the dynamics of extended rod-like bodies in (or associated with) membranes and films. We demonstrate a striking difference between the mobilities in films and bulk fluids, even when the dissipation is dominated by the fluid stress: for large inclusions we find that rotation and motion perpendicular to the rod axis exhibits purely local drag, in which the drag coefficient is algebraic in the rod dimensions. We also study the dynamics of the *internal* modes of a semiflexible inclusion and find two dynamical regimes in the relaxation spectrum.

The mobility of inclusions in membranes is a fundamental physical parameter controlling a number of cellular processes. Since inclusions such as proteins [1, 2] or "rafts" [3, 4] can in many cases be large compared with the constituent lipids of the membrane, they can be viewed as macroscopic objects moving in a continuum fluid environment. The dynamics of these objects in thin films has already been shown to be surprisingly subtle, leading to confusion in the early literature on protein diffusion in cell membranes [5]. This controversy was clarified by Saffman [6], who noted that motion of objects in or attached to a (two dimensional) membrane is never strictly two-dimensional since in-plane momentum induces flows in the surrounding bulk (three-dimensional) fluids due to a viscous coupling of the interface/membrane to the surrounding fluids. That coupling introduces a new length-scale $\ell_0 = \eta_{\rm m}/\eta_{\rm f}$ determined by the ratio of membrane and fluid viscosities, $\eta_{\rm m,f}$. This length determines the degree to which the dissipation is predominantly two- or three-dimensional [5, 6, 7, 8, 9, 13]. As a result, the drag coefficient on a small object in a membrane is a nonlinear function of both its size and the membrane viscosity. For example, the diffusion coefficients of small proteins (linear size $< \ell_0$) in membranes have a weak (logarithmic) dependence on their size.

Here, we examine the motion of rod-like inclusions in viscous films and membranes, as a representative example of a general scheme for the calculation of mobilities of arbitrary extended bodies, which we also present. The generalization of this problem to motion in viscoelastic films is straight-forward. Our work is motivated in part by prospect of computing mobilities of proteins and lipid rafts in lipid bilayers [1, 2], as well as by recent experiments that have demonstrated the possibility of making quantitative rheological measurements of viscoelastic films resembling cellular structures such as the *actin cortex* [9] using tracer particle fluctuations (membrane microrheology). Given its flexibility, this formalism can be adapted to the computation of the mobility of highly complex and irregular interfacial objects such as fractal aggregates[10]. Finally, the driven motion of rods in viscous/viscoelastic films has also been used to determine rheological properties, *e.g.*, of monolayers [11],for which the approach we develop here is important. We also analyze the undulatory motion of semiflexible polymers at a membrane surface.

Our calculation of the hydrodynamic drag on a *rigid* rod of length L, gives two principal results: (i) for small objects (specifically, $L \ll \ell_0$), the drag coefficients become independent of both the rod orientation and aspect ratio; and (ii) for larger rods of high aspect ratio, $\zeta_\perp$ becomes purely linear in the rod length L—*i.e.*, the drag becomes purely local. In contrast, we find that the well-established three-dimensional result $\zeta_\parallel = 2\pi\eta/\ln(AL/a)$ applies for parallel motion in the film, provided that $L \gg \ell_0$. Here, however, the effective rod radius becomes ℓ_0 rather than the physical radius a, when $a \ll \ell_0$. Closely related to (ii), we find that the rotational drag (equivalently diffusion constant) depends purely algebraically on the rod length.

We also calculate the relaxation spectrum of undulation modes of wavelength q^{-1} of a *semiflexible* inclusion of rigidity κ and find a dynamic relaxation time $\tau(q)$ which crosses over from $\tau \sim q^{-3}$ on modes with wavelength less than ℓ_0 to $\tau \sim q^{-4}$ for those longer than ℓ_0. The latter result represents purely local drag, with no additional logarithmic dependence in $\tau(q)$, as there is for bending fluctuations in a bulk fluid.

The starting point of our analysis will be the response of the two dimensional membrane fluid to an in-plane force distribution. This is calculated by solving the coupled equations for in-plane and out of plane fluid motions taking into account incompressibility [13] of both the bulk and the membrane leading to an expression for the in-plane velocity $v_\alpha(\mathbf{x})$ at position $\mathbf{x}$ resulting from a point force $f_\beta(\mathbf{x}')$ at *another* point $\mathbf{x}'$: $v_\alpha(\mathbf{x}) = \alpha_{\alpha\beta}(\mathbf{x}-\mathbf{x}')\, f_\beta(\mathbf{x}')$. The response function $\alpha_{\alpha\beta}(\mathbf{x})$ is given in closed form as

$$\alpha_{\alpha\beta}(\mathbf{x}) = \alpha_\parallel(|\mathbf{x}|)\,\hat{x}_\alpha\hat{x}_\beta + \alpha_\perp(|\mathbf{x}|)\,[\delta_{\alpha\beta} - \hat{x}_\alpha\hat{x}_\beta], \quad (1)$$

where the scalar functions $\alpha_\parallel, \alpha_\perp$ of the distance between the point of the force application and the measurement of the velocity field are given by:

$$-4\eta_m i\omega\alpha_\parallel(x,\omega) = \frac{\mathbf{H}_1(z)}{z} - \frac{2}{\pi z^2} - \frac{Y_0(z)+Y_2(z)}{2} \quad (2)$$

$$-4\eta_m i\omega\alpha_\perp(x,\omega) = \frac{z\mathbf{H}_0(z)-\mathbf{H}_1(z)}{z}+\frac{2}{\pi z^2}-\frac{Y_0(z)-Y_2(z)}{2}, \quad (3)$$

where the $\mathbf{H}_\nu$ are Struve functions[14], and the Y_ν are Bessel functions of the second kind. Here, $z = |\mathbf{x}|/\ell_0$ is the distance between the point of force application and the membrane velocity response measured in the flat film in units of ℓ_0.

To parameterize this geometry of the rod of length L and circular cross-section a, we define the dimensionless aspect ratio $\rho = L/a$. There are three independent drag coefficients to determine in the problem. The in-plane translational mobility tensor, $\mu_{\alpha\beta}$ (and consequently, its inverse, the drag $\zeta_{\alpha\beta} = \mu^{-1}_{\alpha\beta}$) is defined by

$$v^{\rm rod}_\alpha = \mu_{\alpha\beta}F^{\rm rod}_\beta, \quad (4)$$

where $v^{\rm rod}_\alpha$ is the $\alpha^{\rm th}$ component of the velocity of the rod and $F^{\rm rod}_\beta$ is the $\beta^{\rm th}$ component of the total force applied to the rod (at its center) and $\alpha,\beta \in \{1,2\}$. In-plane rotational symmetry and inversion of the rod imply that the mobility tensor has the form: $\mu_{ij} = \mu_{||}\hat{n}_i\hat{n}_j + \mu_\perp(\delta_{ij}-\hat{n}_i\hat{n}_j)$. Here $\mu_\perp$ and $\mu_\parallel$ are the mobility of the rod dragged perpendicular to and parallel to its long axis (oriented along the $\hat{n}$ direction) respectively. In addition to these two independent translational mobilities, there is also one rotational mobility, $\mu_{\rm rot}$ linking the angular velocity of the rod to the torque applied to that rod about its center of inversion symmetry.

We solve the problem by two complementary methods useful for the regimes of small and large aspect ratios respectively. For small ρ, we use a 2-d analogue of the Kirkwood approximation [15] to model the continuous rod by a series of discs subject to point forces at their centers. This method becomes rather cumbersome when $\rho \gg 1$, but here we may proceed by a second approximation that assumes the rod to be infinitely thin. In both cases, we restrict our attention to the limit $a \ll \ell_0$. Below, we illustrate both methods by a calculation of the transverse drag coefficient with the understanding that the longitudinal and rotational drag proceed analogously.

The linearity of the underlying low-Reynolds number hydrodynamics allows to use superposition. Specifically, we replace the rod of length L and cross–sectional radius a by a set of $N+1$ disks of radius a and interdisk separation b chosen so that the total length of the rod is preserved, i.e. $L = Nb + 2a$. We choose the number of disks to be maximal consistent with a given aspect ratio and the non-interpenetrability of the disks.

Our strategy for computing the drag on the rod involves setting the rod in uniform motion with unit velocity by imposing some set of forces $\mathbf{f}^{(i)}$, $i = 1,\ldots,N+1$ on the $N+1$ disks making up the rod. We can use the response function to compute the velocity field for a given collection of point forces $v^{(i)}_{\parallel,\perp} = \sum_{i=1}^{n+1}\alpha^{(ij)}_{\parallel,\perp}f^{(j)}_{\parallel,\perp}$. However, we must demand that all the disks have the *same* velocity and thereby determine the forces applied to them. To enforce this constraint, we invert the matrix $\alpha^{(i,j)}_{\parallel,\perp}$. The drag coefficient is then, $\zeta_{\perp,\parallel} = \sum_{i,j=1}^{n+1}\left(\alpha^{-1}_{\perp,\parallel}\right)^{(i,j)}$.

For large N, *i.e.* high aspect ratio rods, the matrix inversion becomes difficult. To study that limit, one can assume an infinitely thin rod. Then, the velocity field at the point $\mathbf{x}$ due to a continuous distribution of force densities along the rod, $\mathbf{f}(x\hat{x})$ that lie along the $\hat{x}$-axis from $x = -L/2$ to $x = L/2$ takes the form

$$v_\alpha(\mathbf{x}) = \int_{-L/2}^{L/2}\alpha_{\alpha\beta}(\mathbf{x}-p\hat{x})\,f_\beta(p\hat{x})\,dp\,. \quad (5)$$

As before, we impose a unit velocity field on the rod and determine the force density required to effect this result, $\mathbf{f}(\mathbf{x})$. The inversion of Eq. 5 proceeds by first expanding the linear force density in Legendre polynomials $P_n(x)$ writing

$$f(x) = \sum_{n=0}^{N} c_{2n}P_{2n}(2x/L) \quad (6)$$

where the coefficients are as yet unknown. Since the Legendre polynomials form a complete set on the interval -1 to $+1$, any physical force density can be expressed as in Eq. 6 provided N be taken to infinity. In practice, we find excellent numerical results even when truncating this sum to just the first five terms, while taking into account the symmetry of the force distribution about the center of the rod.

We now impose the unit velocity condition at a finite set of points $0 \le p_i \le L/2$ along the rod since if we truncate the Legendre function expansion of the force density at N, we can impose the velocity condition at a maximum of N points without creating an overdetermined system of equations. Thus we require that $\mathbf{v}(p_i\hat{x}) = 1, \text{for}\, i = 1,\ldots,N$. Now finding the force distribution along the rod requires only the inversion of an $N\times N$ matrix, $\mathcal{N}_{ij}$ whose components are defined by

$$\mathcal{N}_{ij} = \int_{-L/2}^{L/2}\alpha(\hat{x}p_i - z\hat{x})\,P_j(2z/L)\,dz. \quad (7)$$

Finally, the total force on the rod is found by reconstructing the force density from its Legendre polynomial expansion and integrating the resulting expression over the entire rod. That force density is given by Eq. 6 where the coefficients, c_k are determined using the rod's unit velocity condition enforced at a discrete set of points along with the inverse of the matrix defined in Eq. 7. Thus we find $c_k = \sum_{i=1}^{N}\mathcal{N}^{-1}_{ki}$. Due to the orthonormality of the Legendre polynomials, the total force is given entirely by the coefficient of the zeroth Legendre polynomial,and the total torque in the case of rotations is given by the

coefficient of the first odd Legendre polynomial, c_1. Numerically, we find a variation of less than a percent in the drag coefficient in all cases, so long as $N > 2$. Here, we report our results for $N = 5$. To check for consistency, we compared our results from this method and the Kirkwood approximation; for thin rods, we find excellent agreement.

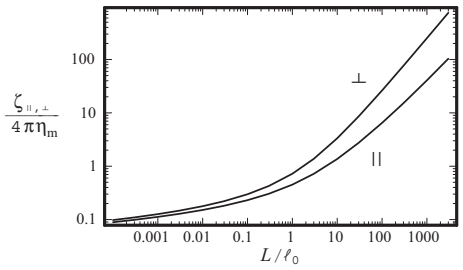


FIG. 1: Parallel (||) and perpendicular ⊥ drag coefficients for thin rods (*i.e.* high aspect ratio) of various lengths. For short rods both the parallel and perpendicular drag coefficients approach the Saffman-Delbrück result. The divergence between these two drag coefficients at long lengths reflects the absence of the hydrodynamic cooperativity in perpendicular case.

The analogous calculation can be made for the drag on the rod moving in a direction perpendicular to its long axis. The two drag coefficients (parallel and perpendicular) converge rapidly for rods of length $L < \ell_0$, while their difference grows monotonically with increasing rod length for $L > \ell_0$. This results stands in contrast to the case of motion in bulk fluids, where the two drag coefficients differ by a constant multiple.

We plot the parallel and perpendicular drag coefficients for thin rods as a function of their length, L/ℓ_0 in reduced units in Figure 1. The equality of the two drag coefficients when all dimensions of the rod are small compared to ℓ_0 reflects the effective shape and size independence of the Saffman-Delbrück result. For rods longer than this crossover length, these two drag coefficient diverge from each other while they both become more strongly length dependent.

To understand this peculiarity of interfacial drag, we note two points. First, for long rods ($L > \ell_0$), the parallel drag in the film is essentially unchanged from the bulk, three-dimensional drag, in that $\zeta_\parallel = \frac{2\pi\eta L}{\ln(0.43L/\ell_0)}$, where the prefactor in the logarithm has been determined to within 1%. Comparing with the result for drag of a rod in a bulk fluid, we see that the effective radius of the rod is now of order ℓ_0 (for $a \ll \ell_0$). Given that ℓ_0 corresponds to a length scale over which interfacial momentum densities flow into the bulk fluid due to the viscous coupling between the two, the system does not effectively resolve length scales smaller than ℓ_0 so the small dimension of the rod is replaced by this length. At large length scales (compared to ℓ_0) the fluid velocity field around the rod in parallel drag is the same as for rod motion in the bulk fluid, *i.e.* in both cases there should have been no flow from the plane of the interface into the subphase.

The case of perpendicular motion of long rods, on the other hand, is qualitatively very different. Here we find $\zeta_\perp = 2\pi\eta L$. For this case, the fluid flow field for a rod in bulk is inconsistent with the flow restrictions imposed by the presence of the interface. In 3d, there would be a non-vanishing two-dimensional divergence of velocity field restricted to the plane of motion of the rod. Now, the in-plane incompressibility of the interface requires that the fluid velocity field extend over distances comparable to the rod's largest dimension L. The standard hydrodynamic coupling of portions of the rod, which gives rise to the logarithm in the drag is not present resulting in a drag coefficient that is purely linear in rod length. In other words, the drag is effectively *local* or "free-draining" in character. In three dimensions, in contrast, there is a length-independent ratio of two between the parallel and perpendicular drag coefficients because neither is free-draining: $\zeta_\parallel^{3d} = \frac{2\pi\eta L}{\ln\left(\frac{AL}{a}\right)}$ and $\zeta_\perp^{3d} = 2\zeta_\parallel^{3d}$.

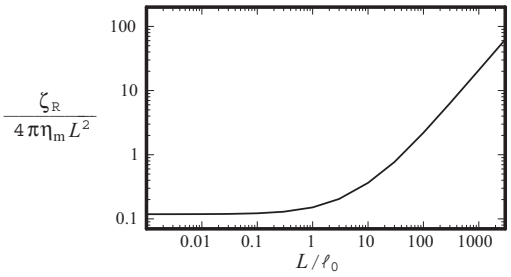


FIG. 2: The rotational drag coefficient of a rod of infinite aspect ratio plotted versus the length of the rod.

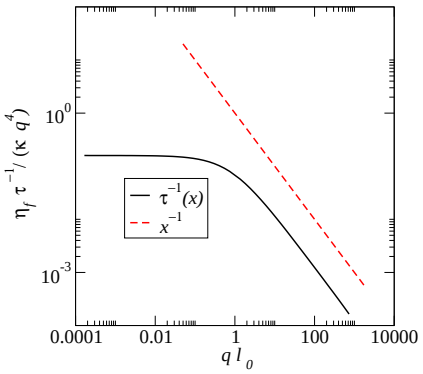


FIG. 3: The decay rate vs wavevector of transverse fluctuations of a semiflexible rod embedded in the interface. The decay rate scaled by q^4 is wavevector–independent for purely local drag (small q regime). Nonlocal hydrodynamic interactions along the rod reduce the decay rate in a manner analogous to [16] in the larger q regime.

The calculation of the rotational drag coefficient proceeds analogously to those of the perpendicular and parallel drag coefficients. We plot the rotational drag coefficient divided by L^2 for a rod of infinite aspect ratio as a function of the reduced length in figure 2. The essen-

tial feature of this plot is that rotational drag coefficient scales as L^2 for rods smaller than ℓ_0 and then as L^3 for rods longer than this natural length. Thus, we find purely algebraic behavior in both limits.

Finally, to study the internal mode dynamics of a semi-flexible inclusion, we consider the small transverse fluctuations of a an infinitely thin, almost rod-like filament oriented along the x axis parameterized by $(x, r(x,t))$. With no slip boundary conditions on the inclusion we have a dynamical equation for $r(x)$ to linear order,

$$\partial_t r(x,t) = \int dx' \boldsymbol{\alpha}(x-x',0) \cdot \left(0, -\kappa \partial_x^4 r\right) + \eta(x,t) \quad (8)$$

where the thermal fluctuations $\eta(x,t)$ are chosen to satisfy the Fluctuation-Dissipation Theorem. Expanding in modes of wavenumber q, we obtain a relaxation spectrum of transverse correlations given by

$$\langle \tilde{r}(q,t)\tilde{r}(q,0)\rangle = \frac{2k_BT}{\kappa q^4} \exp\left[-t/\tau(q)\right] . \quad (9)$$

where $\tau^{-1}(q) = \dfrac{2\kappa q^4}{\eta_m} \displaystyle\int_q^\infty \frac{dx}{2\pi} \frac{q^2}{x^2(x^2-q^2)^{1/2}(x+\ell_0^{-1})}$. We have obtained a *complicated* but *closed form* expression for $\tau(q)$ that is plotted in figure 3. It is simple in the two limits of $q\ell_0 \ll 1$, $q\ell_0 \gg 1$ where $\tau^{-1}(q \ll \ell_0^{-1}) \simeq \dfrac{\kappa q^4}{\pi\eta}$ and $\tau^{-1}(q \gg \ell_0^{-1}) \simeq \dfrac{\kappa q^3}{4\eta_m}$ respectively. At short scales we find the dimensionally reduced analogue of the hydrodynamic relaxation spectrum of fluid membranes ($D=2$ dimensional manifold embedded in $D+1$ dimensions) [16] (we consider $D=1$). Here though, the 'long-range' hydrodynamic coupling crosses over to a purely *local* friction on the longest length scales [17].

In summary, we have calculated the translational and rotational hydrodynamic drag on a rod moving at low Reynolds number in a viscous film coupled to viscous sub- (and/or) superphase. When the dimensions of the rod are small ($\ll \ell_0$), the dissipation is governed primarily by the film, and the drag is insensitive to orientation and aspect ratio, and only weakly (logarithmically) dependence on size[6]. We find, surprisingly, that in the limit of a long rod, the drag for motion perpendicular to the rod axis exhibits purely local drag per unit length. Thus, in contrast with motion in 3d fluids, there are no long-range hydrodynamic effects for long rods, even though the dissipation occurs entirely in the fluid. A similar observation applies to rotational motion, and for the relaxation spectrum of the long wavelength modes of a fluctuating filament or semi-flexible polymer in a viscous film. This is because, although the dissipation is governed primarily by the fluid, the film (along with its assumed incompressibility and no-slip conditions) imposes a very different boundary condition on the flow from what we would have in a bulk fluid alone. This added condition not only *increases* the drag for perpendicular motion relative to that without the film present, but results in purely local, or free-draining drag dynamics. In contrast, since the new boundary conditions *are* consistent with the standard flow field for parallel motion, we find quantitative agreement with the parallel mobility in a bulk fluid when the film's viscosity becomes irrelevant (small ℓ_0). Finally, we note that the methods developed here constitute a highly adaptable framework to compute the mobility of arbitrary extended, irregularly shaped objects embedded in a viscous membrane or interface.

[1] R.A. Stein, E.J. Hustedt, J.V. Staros, and A.H. Beth Biochem., **41**, 1957 (2002).

[2] P.J.R. Spooner, R.H.E. Friesen, J. Knol, B. Poolman, and A. Watts Biophys. J., **79**, 756 (2002).

[3] K. Simons and E. Ikonen, Nature **387**, 569 (1997).

[4] A. Pralle, P. Keller, E.L. Florin, K. Simons, and J.K.H. Horder J. Cell Biol.,**148**, 997 (2000).

[5] B.D. Hughes, B.A. Pailthorpe and L.R. White, J. Fluid Mech., **110**, 349 (1981).

[6] P.G. Saffman, P. Natl Acad Sci USA **72**, 3111 (1975). See also H.A. Stone J. Fluid Mech., **409** 165 (2000).

[7] D.K. Lubensky and R.E. Goldstein Phys. Fluids **8**,843 (1996).

[8] A. Ajdari and H.A. Stone J. Fluid Mech., **369**, 151 (1998).

[9] E. Helfer, S. Harlepp, L. Bourdieu, J. Robert, F.C. MacKintosh, and D. Chatenay, Phys. Rev. Lett. **85**, 457 (2000); E. Helfer, S. Harlepp, L. Bourdieu, J. Robert, F.C. MacKintosh, and D. Chatenay, Phys. Rev. E **63**, 021904 (2001).

[10] P.B. Warren Nuovo Cimento D **16**, 1231 (1994); Private communication with A.D. Dinsmore and T.P. Russel.

[11] C.F. Brooks, G.G. Fuller, C.W. Frank, and C.R. Robertson Langmuir **15**, 2450 (1999); J.Q. Ding, H.E. Warriner, J.A. Zasadzinski, and D.K. Schwartz Langmuir **18**, 2800 (2002).

[12] H. Lamb *Hydrodynamics* 6^{th} *ed.* Dover Publications, New York (1945).

[13] Alex J. Levine, F.C. MacKintosh, PRE **66**, 061606 (2002).

[14] *Handbook of Mathematical Functions with Formulas, Graphs, Mathematical Tables*, eds. M. Abromowitz and I.E. Stegun National Bureau of Standards, Washington D.C., (1964).

[15] See, for example Chapter 8 in M. Doi and S.F. Edwards *The Theory of Polymer Dynamics*, Clarendon Press, Oxford (1986).

[16] F. Brochard and J.F. Lennon, J. Phys. (France) **36**, 1035 (1979).

[17] That the drag coefficient per unit length of an oscillating line becomes independent of wavelength in the long wavelength limit was noted in Ref. [7].